Ultrawideband TEM Horn Circular Array

Mohamed A. Elmansouri, Jaegeun Ha, and Dejan S. Filipovic

***Abstract*— An eight-element circular array of miniaturized combined TEM horn and loop elements for joint frequency and time operation is presented. The use of such ultrawideband and compact directional element leads to stable wideband radiation patterns with moderate gain for omnidirectional phase mode 0 of operation. Moreover, a directional mode enabled by simply exciting specific element(s) in the array is also demonstrated. Obtained directional beams can be steered to a desired direction in horizontal plane simply by exciting an appropriate element. Low-dispersion of the utilized element permits distortionless pulse radiation for both modes of operation. The performance of the proposed array is characterized computationally and experimentally in frequency and time domains for both modes. The fabricated circular array has VSWR < 2, good omnidirectional (wobble on the wave (WoW) < 5dB) and directional (front to back ratio (F/B) > 10dB) radiation characteristics, nominal gain > 6dBi, cross polarization level < -15dB, and excellent time-domain performance with high fidelity factor over more than two octaves.**

***Index Terms*— Circular array, fidelity factor, omnidirectional radiation, TEM horn, time-domain, wideband operation.**

I. Introduction

Circular arrays have long been used in different communication, broadcast, and navigation systems to obtain full 360° azimuthal coverage [1]-[3]. Multimoding [2]-[3], processing of phase-steered directional beams through 360° in azimuthal plane with minimal change in side lobe levels and beamwidth [1], nulls placement/steering [4], and potential wideband operation make the circular antenna arrays viable candidates for direction finding, electronic support measures, radar, and smart antenna applications [1]-[4]. The theory and the design of circular arrays are well-established in literature [1]-[3], [5]-[6]. Several circular array topologies employing omnidirectional [5] and directional elements [6] are proposed and analyzed in terms of different phase and amplitude excitations. To achieve consistent wideband operation, broadband antenna elements such as bicone/discone [7], Vivaldi [8], log-periodic, and TEM horn antennas [9]-[10] are utilized. Large number of elements (e.g. 16 elements or more) is used to guarantee good omnidirectional patterns over wide bandwidth [1],[11] leading to excessively large and complex arrays which is impractical for many modern compact transceivers. In this paper, a miniaturized transverse electromagnetic (TEM) horn antenna [12] is considered as an array element able to reduce the size of the wideband array and provide good joint time and frequency operation. The small size and wideband directional characteristics of the utilized element allow for compact array realization while maintaining excellent mode 0 omnidirectional patterns over more than two octaves of bandwidth. Note that higher-order modal excitations [1], [3] are out of scope of this paper.

In addition to omnidirectional mode of operation, the synthesis of electronically steered directional beams over the entire azimuthal plane has also been studied [1], [6], [11]. However, attaining this feature requires the change of both the amplitude and phase of all elements resulting in more complicated beamformer network than that of linear arrays [6]. Herein, a simpler implementation of reconfigurable omnidirectional/directional operation [13] is achieved by simply exciting a specific TEM horn(s) in the array to cover a certain direction while disconnecting the other elements. Each element provides consistent sectorial coverage permitting a full beam scan operation in azimuthal plane.

This paper also discusses the extension of the circular array functionality to the time domain in order to achieve simultaneous time and frequency domain operation. Pulsed circular arrays are attractive for many ultrawideband (UWB) applications; in particular, indoor radio-navigation, automotive radars, and surveillance [14]-[15]. Herein, the wideband low-dispersion characteristics of TEM horn are utilized to achieve high quality time-domain performance. The fidelity factor and energy patterns are investigated to assess the proposed circular array performance in time domain for the omnidirectional and directional modes of operation. Finite element and finite integration methods as implemented in Ansys HFSS and CST-Microwave Studio are used to compute the frequency- and time-domain performances. Theory and measurements show that the proposed eight-element TEM horn array can operate over more than 4:1 bandwidth with VSWR < 2, moderate gain, stable omnidirectional/directional characteristics, and fidelity factor > 90% over a wide field of view.

This paper is organized as follows: Section II reviews the main design parameters, outlines their impact on the array's performance, and presents the proposed design. Section III discusses the measured and simulated omnidirectional and directional frequency-domain performances of the realized array. Finally, the time-domain performance is discussed in Section IV.

II. Circular Array Design

The far-field pattern of a circular array formed by N equally spaced elements located on a circle of radius a in the xy- plane, as shown in Fig. 1 inset, can be approximated as [3],

$$E_{array} = \sum_{n=1}^{N} E_e(\theta, \varphi - \varphi_n)|I_n| e^{j\left(\left(\frac{Nd}{\lambda}\right)\sin\theta\cos(\varphi-\varphi_n)+\beta_n\right)} \quad (1)$$

where $\varphi_n = 2\pi n/N$ (n=1,2,…,N) is the angular position of the n^{th} element and $|I_n|e^{j\beta_n}$ denotes its complex excitation coefficient, $d = 2\pi a/N$ is the arc length interelement spacing, and $E_e(\theta, \varphi - \varphi_n)$ is the field pattern of the n^{th} element placed at an angle φ_n. As seen in the absence of coupling, the far-field radiation of the considered array is determined by:

This work was supported by the Office of Naval Research (ONR) award # N00014-13-1-0537.

The authors are with the Department of Electrical, Computer, and Energy Engineering, University of Colorado, Boulder, CO 80309-0425 USA (e-mail: { mohamed.elmansouri,jaegeun.ha,dejan}@colorado.edu).

This article has been accepted for publication in a future issue of this journal, but has not been fully edited. Content may change prior to final publication. Citation information: DOI 10.1109/TAP.2016.2637871, IEEE Transactions on Antennas and Propagation

element's pattern (E_e), interelement spacing (d), number of elements (N), and the applied excitation ($|I_n|e^{j\beta_n}$). Expression (1) is used to assess the impact of these parameters on the array performance and to determine those with greater likelihood of enabling the desired array performance. Notice that the mutual coupling between the elements is neglected in this analysis.

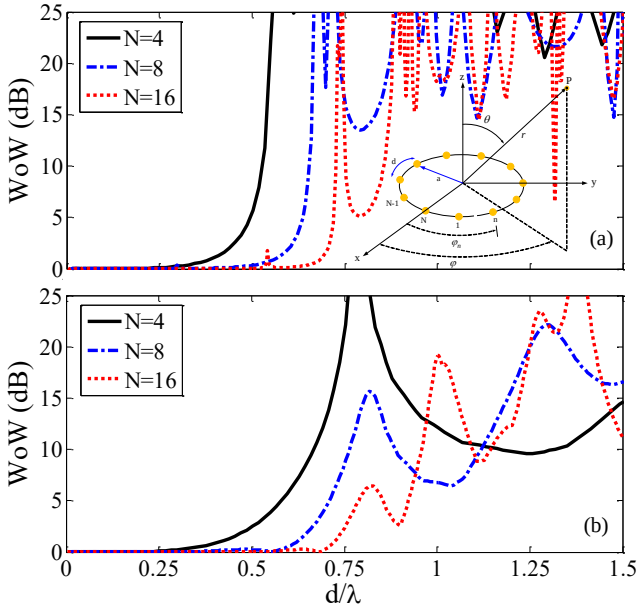

Fig. 1. WoW vs. element spacing in wavelengths for circular arrays with (a) omnidirectional and (b) directional elements for different N.

To determine the impact of the element pattern, the performance of uniform circular arrays employing omnidirectional and directional elements is assessed. For omnidirectional case, $E_e(\varphi) = 1$ is chosen for simplicity. Whereas, $E_e(\varphi) = 1 + \cos\varphi$ is chosen to approximate the radiation of directional element since this could be a realistic approximation for many practical antennas [3],[6]. The studies are conducted for uniformly excited N elements (i.e. $I_n = I_o$, $\beta_n = 0^o$). Omnidirectionality is considered as a main design criterion for this mode of operation. The parameter wobble on the wave (WoW) [16], defined as the maximum variation of the electric field in azimuthal plane at specific elevation angle (see (2)), is used to quantify the circular array's omnidirectionality.

$$WoW = \max\left(E_{array}(\varphi,\theta_0)_{dB}\right) - \min\left(E_{array}(\varphi,\theta_0)_{dB}\right) \quad (2)$$

WoW in xy-plane (θ=90°) is plotted in Fig. 1 for both cases as a function of element spacing. As seen, lower WoW is achieved over wider bandwidth (or for larger interelement spacing) for the array employing directional elements. The deterioration of WoW is due to excitation of the undesired higher-order phase modes which are more pronounced in the case of omnidirectional elements. The use of directional elements also prevents the rapid deterioration of the pattern shape with elevation angles [6], minimizes the near field effects inside the array [3], and enables higher gain as well as better pattern stability over wide bandwidth [6]. The wideband operation of the circular array can be further improved by increasing the number of directional/omnidirectional elements as shown in Fig. 1. Yet, the improvement is more evident in the case of directional elements (see Fig. 1(b)). This comes at expense of increasing the overall array size, cost, and complexity. As seen, to achieve good wideband omnidirectional characteristics, the higher-order harmonics need to be suppressed or mitigated by using directional elements, reducing the interelement spacing (i.e. ideally ka < N/2 or d < 0.5λ), or increasing the number of elements.

Taking into account these design considerations, a compact directional antenna is investigated as an array element. Specifically, a combined TEM horn and loop antenna with crescent slots is designed using the spherical mode theory to combine the fundamental spherical TM and TE modes of the TEM horn and the loop, respectively to simultaneously lower the turn-on frequency and improve gain at the low end [12]. The half-cut of combined antenna with electrical size of $0.188\lambda \times 0.145\lambda \times 0.087\lambda$ at the turn-on frequency is built and integrated with a finite size ground plane. The photograph of the fabricated antenna with denoted dimensions is shown in Fig. 2. Measurements show that the 2:1 VSWR turn-on frequency is at 0.87GHz. The design procedures and performance of this antenna are discussed in [12]. The fabricated uniform circular array is also shown Fig. 2. The array is composed of eight half-cut combined TEM and loop antennas fabricated over a 35cm-diameter circular ground plane. N=8 is chosen as a compromise between good far-field performance and size/complexity. The physical radius of the realized circular array (from the array center to the end of each element) is 12cm.

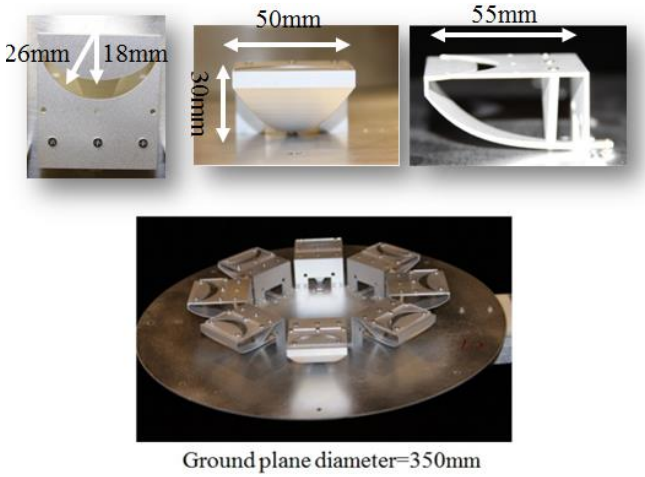

Fig. 2. Photographs of the fabricated combined antenna and circular array over a ground plane.

III. Frequency-Domain Performance

Measured and simulated active VSWRs of the eight elements for uniform excitation (i.e. phase mode 0) are shown in Fig. 3. Similar VSWRs are measured by the virtue of the array symmetry. A turn-on frequency of 0.80 GHz and VSWR < 2 are measured over almost 7.5:1 bandwidth. The utilized feeding network is the commercial off-the-shelf (COTS) 8-way power splitter (mini-circuits-ZN8PD1-63W+ [17]). It operates from 0.5-6GHz with amplitude and phase imbalances <0.5dB and 4°; respectively, isolation >20dB, and insertion loss <1.5dB. The

array is modeled in Ansys-HFSS and good agreement with measurement is observed. Notice that the simulation in Fig. 3 is shown only for one element; the other elements have similar VSWR.

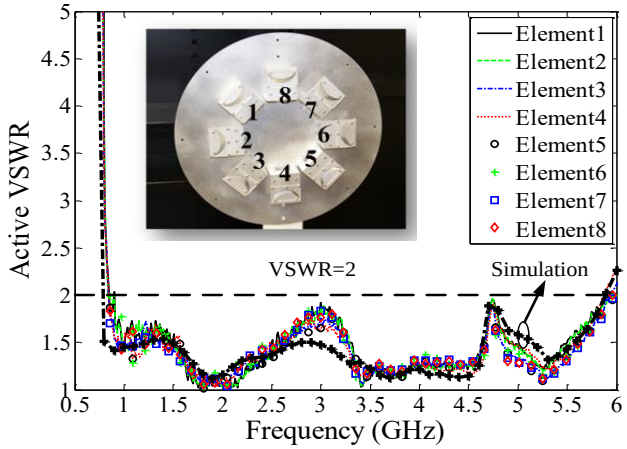

Fig. 3. Measured and simulated active VSWRs of the proposed circular array in the case of uniform excitation.

For the directional mode of operation (i.e. when only one element is excited and other elements are terminated with matched loads), good impedance match (VSWR < 2) is measured over wide bandwidth as shown in Fig. 4. VSWR is deteriorated around 1.24GHz which is not seen in the case of the stand-alone combined antenna shown in the inset. This is due to the coupling with other elements (i.e. parasitic elements) at these frequencies as depicted in Fig. 5. Similar mutual couplings are observed for other elements due to the geometrical symmetry of the circular array. Mutual coupling decreases as the frequency increases leading to less detrimental effects on the impedance match. Notice that the mutual coupling has less impact in the case of omnidirectional mode due to the symmetry [1]. In fact, the mutual coupling helps to slightly lower the turn-on frequency of the array ($f_{turn-on} = 0.8GHz$) compared to the single element ($f_{turn-on} = 0.87GHz$).

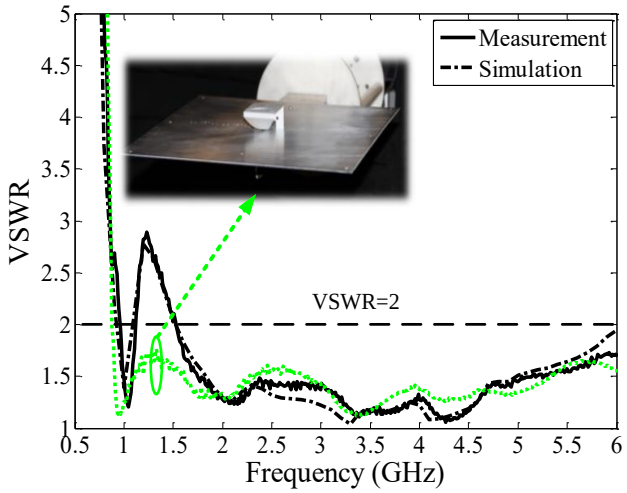

Fig. 4. Measured and simulated VSWRs of one element in the proposed circular array (other elements are terminated with 50 Ω loads). Also shown is the VSWR of a standalone antenna displayed in the inset.

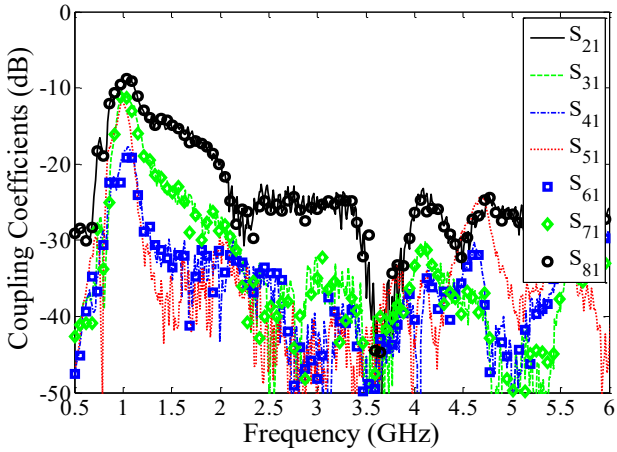

Fig. 5. Measured mutual coupling between element 1 and all other array's elements.

A. *Omnidirectional Mode Far-Field Performance*

The measured radiation patterns of the uniformly-excited circular array are shown in Figs. 6(a) and (b) at elevation cuts θ=30° and 90°, respectively. As seen, omnidirectional radiation patterns are measured with low WoW and low cross polarization level over more than 5:1 bandwidth. However, as the elevation angle increases the omnidirectionality degrades; especially at higher frequencies (see Fig. 6(b)). This is due to the radiation of higher-order modes and the element beamwidth variation which are more pronounced at higher elevation angles and frequencies. Contour plot of the realized array WoW versus the elevation angles and frequency is shown in Fig. 7. The WoW degradation in the case of higher elevation angle is clearly demonstrated. Yet, wideband operation with low WoW (WoW < 3dB) can still be achieved over wide field of view.

The measured and simulated peak realized gain of the uniform circular array is shown in Fig. 8. The gain is greater than 5dBi over most of the operating bandwidth (starting from 1GHz). The drop in the gain around 3GHz is due to the effective radiation of modes ±8 which are the dominant higher order modes in uniformly excited eight-element circular array [3]. Good agreement between measurement and simulation is obtained.

B. *Directional Mode Far-Field Performance*

The measured H-plane (θ=90º) radiation patterns of the array elements when individually excited are shown in Fig. 9. Each element has a sectorial coverage in azimuth with directional pattern over wide range of elevation angles. Low-cross polarization and good F/B ratio are also measured. Elements patterns are deteriorated at the low end due to the finite-size ground plane and asymmetric positioning of elements. Using a larger ground plane will noticeably improve the array's performance. Although the variation of the beamwidth with frequency degrades the coverage at some locations in azimuthal plane, a good beam steering operation can still be achieved over 360º in azimuth by rotating the excitation. Furthermore, the obtained patterns can be combined in different ways in order to achieve certain radiation characteristics in a specific direction at the expense of increased beamformer complexity. The E-plane patterns are squinted due to the finite-size ground plane.

This article has been accepted for publication in a future issue of this journal, but has not been fully edited. Content may change prior to final publication. Citation information: DOI 10.1109/TAP.2016.2637871, IEEE Transactions on Antennas and Propagation

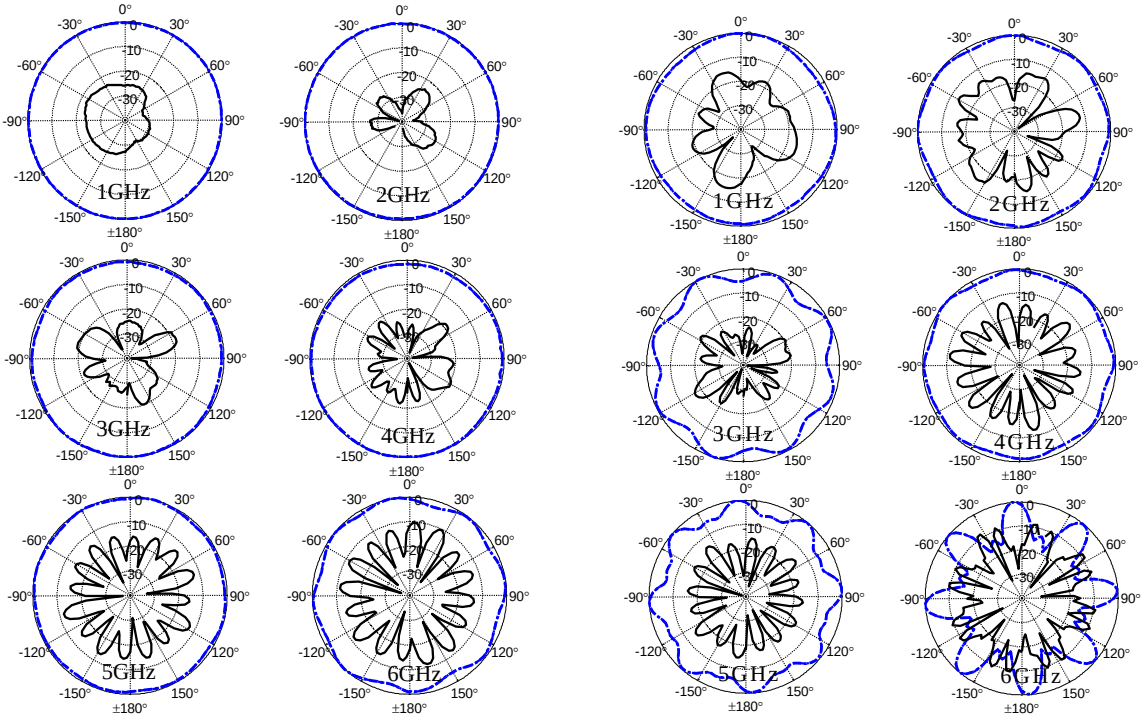

Fig. 6. Measured in-band omnidirectional patterns of the proposed circular array at elevation angle (θ) of (a) 30° and (b) 90°.

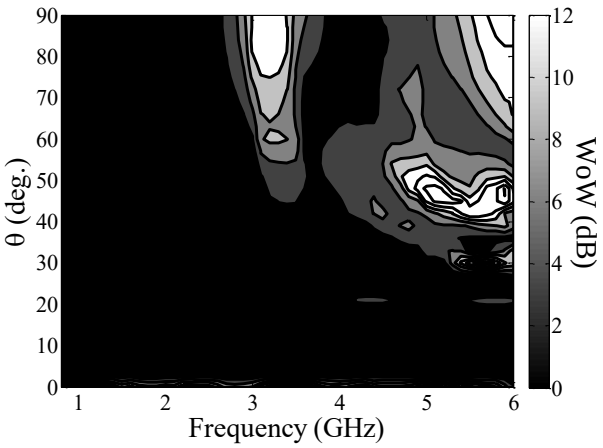

Fig. 7. Contour plot of measured WoW of the proposed circular array versus elevation angles and frequency.

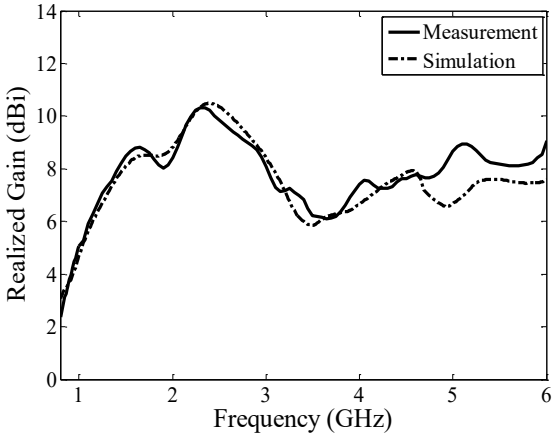

Fig. 8. Measured and simulated peak realized gain of the proposed circular array operating in the omnidirectional mode.

The cross-polarized fields are below -20dB over the operating bandwidth. The parasitic elements (i.e. unexcited elements in the array) have minimum effects on the radiation characteristics in this mode of operation.

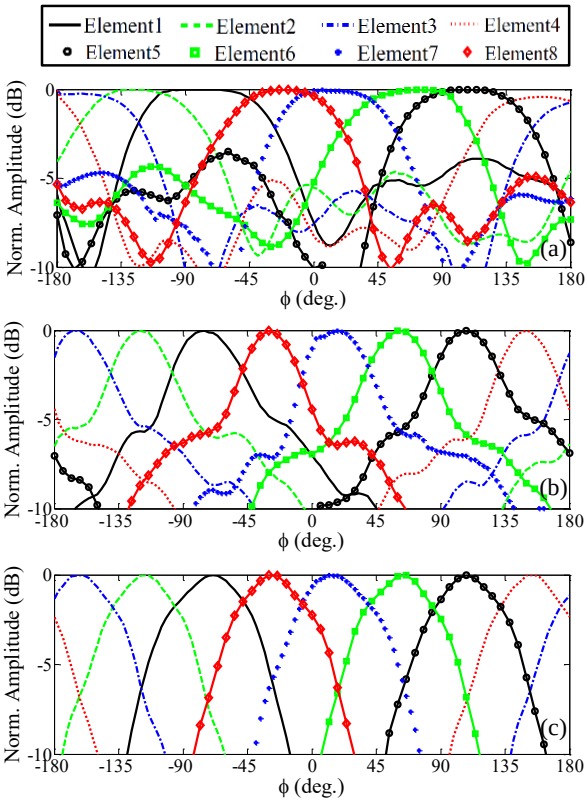

Fig. 9. Measured H-plane directional patterns of the proposed circular array when each element is excited individually at (a) 1GHz, (b) 2GHz, and (c) 4GHz.

This article has been accepted for publication in a future issue of this journal, but has not been fully edited. Content may change prior to final publication. Citation information: DOI 10.1109/TAP.2016.2637871, IEEE Transactions on Antennas and Propagation

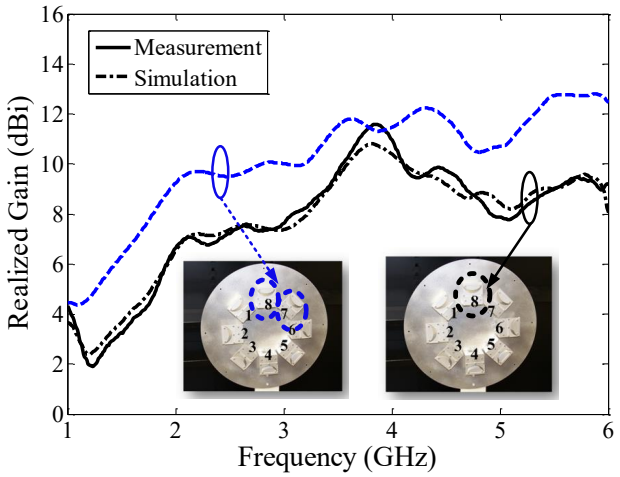

Fig. 10. Peak realized gain of the proposed circular array when one element or two elements are simultaneously excited (as shown in the inset).

The measured and simulated peak realized gains when one element is excited in the proposed circular array are shown in Fig. 10. The nominal gain is greater than 4dBi and it can be further improved by uniformly exciting two adjacent elements. As seen, up to 3dB gain enhancement is achieved by exciting two elements as depicted in the inset of Fig. 10. As mentioned, increasing the ground plane size improves the performance particularly at the low end [12].

IV. Time-Domain Performance

The time-domain performance of the proposed array is also characterized. To do so, the transfer function of each antenna element in the array is determined first at different directions using the two-antenna measurement technique following similar procedures as in [12],[18]. Once the transfer function is measured, the radiated time-domain fields $\vec{e}_i(t)$ are obtained by multiplying the input pulse spectrum with antenna transfer function. The result is then transferred to time domain using the inverse fast Fourier transform (IFFT). Time-domain simulation is conducted using CST-MWS transient solver. The total radiated field of the circular array in the omnidirectional mode is the coherent sum of field strengths of individual elements. The fidelity factor [18] and energy patterns [19] are used to describe the performance of the proposed array in time-domain. For narrowband frequency-domain applications, the power patterns are usually used to describe the array radiation and beam scan; since the scanning is required only at specific frequencies. This is not suitable in the case of UWB applications where the array's operation expands over wide bandwidth; thus, the energy pattern definition [19] is used herein to assess the time-domain energy intensity of the proposed array at a specific direction.

The utilized input pulse is the second derivative Gaussian pulse [20],

$$v_t(t) = \left(\frac{1}{\sqrt{2\pi}\sigma^3} - \frac{(t-t_o)^2}{\sqrt{2\pi}\sigma^5}\right)\exp\left(\frac{-(t-t_o)^2}{2\sigma^2}\right) \quad (3)$$

where t_o is the time shift (chosen to be 0.5 ns), and σ is the parameter that controls the pulse width. For herein study, σ value of 80ps is used to achieve power spectral density with 5:1 10dB-bandwidth from 1GHz to 5GHz. The shape of the input pulse is shown in the inset of Fig. 11(a).

A. Omnidirectional Mode

The radiated pulses for the omnidirectional mode (i.e. when all elements are excited with the same pulse without applying any time delay) are obtained using the aforementioned procedure. The corresponding measured and simulated radiated pulses at φ=0º in xy-plane are shown in the inset of Fig. 11(a). As seen, pulses with a shape almost identical to the input pulse shape and low ringing are radiated. The fidelity factor and energy patterns, shown in Figs. 11 (a) and (b); respectively, demonstrate good time-domain performance. Fidelity factor >0.83 (max. of 0.96) is achieved over 360º in azimuth. The variation in energy pattern is less than 2dB in a designated plane indicating excellent time-domain omnidirectionality. The dips in fidelity factor and energy pattern are periodic with a period of ~ 45°. These dips exist due to slight destructive interference between elements' fields in time domain leading to some pulse distortion.

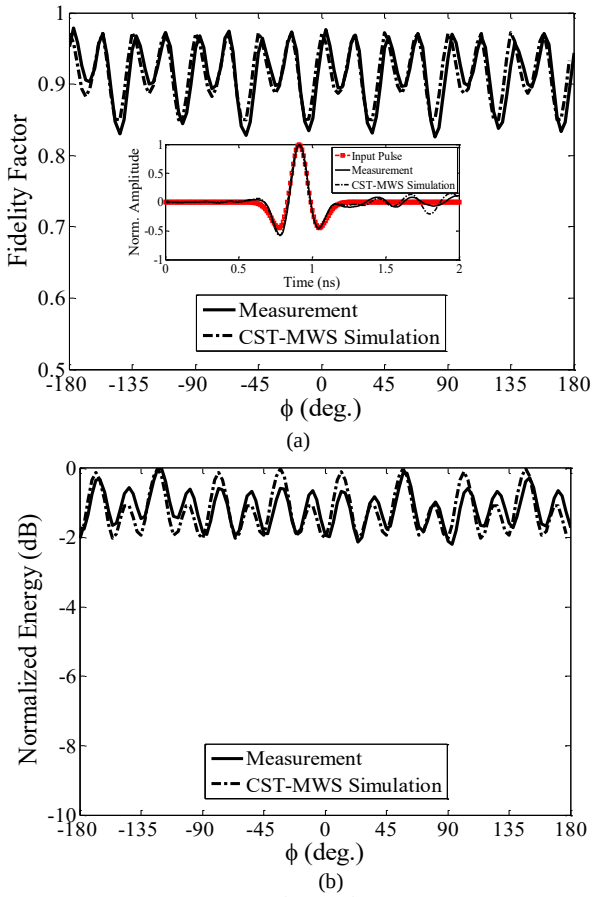

Fig. 11. Measured and simulated (a) fidelity factors and (b) energy patterns of the proposed circular array operating in omnidirectional mode. Measured and simulated radiated pulses at φ=0º are also shown in the inset.

B. Directional Mode

The fidelity factor and energy pattern of each element in the directional mode of operation are shown in Figs. 12(a) and (b); respectively. As seen, high fidelity factor and symmetric energy patterns with no side lobes are obtained for all elements

indicating excellent time-domain performance. Specifically, each element has 45° azimuthal patterns with 0.96 fidelity factor thus enabling high-quality time-domain coverage. Good time-domain performance is also observed at different elevation angles.

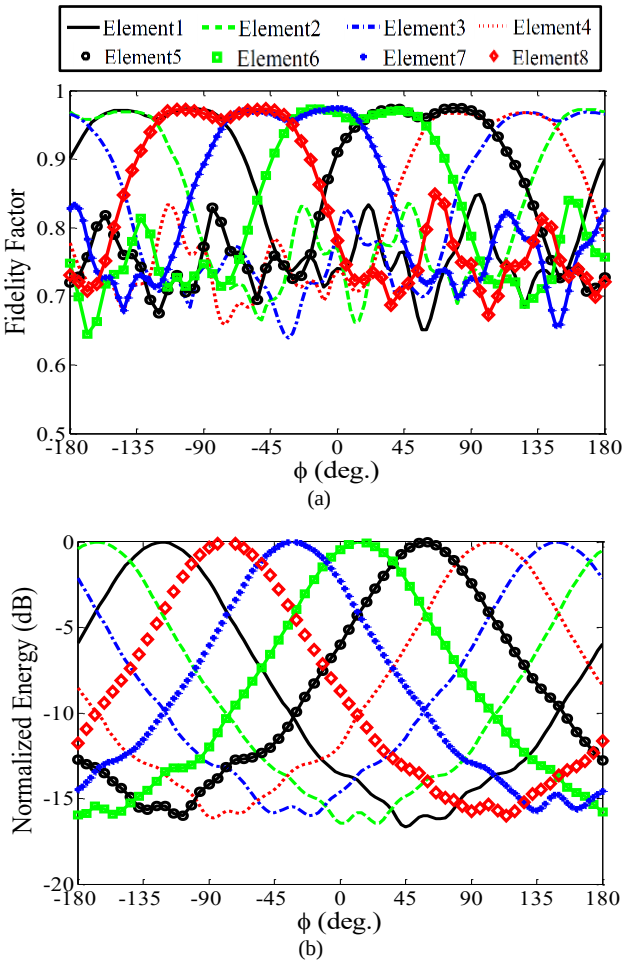

Fig. 12. Measured (a) fidelity factors and (b) energy patterns of the proposed circular array when each element is excited individually.

For both modes of operation, excellent time-domain performance is obtained as a result of utilizing low-dispersion UWB radiator such as the combined TEM horn and loop antenna. The demonstrated omnidirectional time-domain radiation with low amplitude variation and high pulse fidelity as well as easily-obtained directional energy patterns make the proposed circular array an excellent candidate for many UWB radar and surveillance applications.

V. Conclusion

Design and performance of eight-element circular array operating well in frequency and time domains are presented. The miniaturized combined TEM horn and loop antenna is used as an array element enabling a compact array design with reasonable number of elements, dual mode operation (i.e. directional and omnidirectional) with good radiation characteristics, multi-octaves bandwidth, and excellent time-domain performance. The directional mode of operation is implemented by simply exciting a specific array's element to cover a certain direction while disconnecting the others. The omnidirectional radiation is obtained by exciting the array elements with equal amplitude and phase in circular array mode 0. The two modes are theoretically and experimentally characterized in frequency and time domains and excellent agreement between the theory and measurement is demonstrated. The proposed TEM horn circular array can operate over more than two octaves with VSWR <2, good gain, stable and consistent omnidirectional/directional characteristics, and excellent time-domain performance over the full field of view. The demonstrated features make the proposed circular array a visible candidate for different time- and frequency-domain applications.

References

[1] D. E. N. Davies, "Circular Arrays," in *The Handbook of Antenna Design*, ch. 12, London Peregrinus, vol. 2, 1983.

[2] R. C. Hansen, *Phased Array Antennas*. New York: Wiley, 1998.

[3] L. Josefsson and P. Persson, *Conformal Array Antenna Theory and Design*. Piscataway, NJ: IEEE Press, 2006.

[4] D. E. N. Davies and M. S. A. S. Rizk, "A broadband experimental null steering antenna system for mobile communications," *Radio Electron. Eng.*, vol. 48, no. 10, pp. 509–517, Oct. 1978.

[5] T-C. Chu, "On the use of uniform circular arrays to obtain omnidirectional patterns," *IRE Trans.Antennas Propag*, vol. AP-7, no. 4, pp. 436–438, Oct. 1959.

[6] T. Rahim, "Directional pattern synthesis in circular arrays of directional antennas", *Ph.D. Dissertation*, London Univ., 1980.

[7] R. Gunnarsson, T. Martin, and A. Ouacha, Asia-Pacific, "Wide-band circular antenna arrays consisting of bicone, semi bicone or bowtie elements," in *Proc. APMC Microw. Conf.*, Dec. 2006, pp. 2074–2077.

[8] K. Alkhalifeh, R. Sarkis, and C.Craeye, "Design of a novel 3D circular Vivaldi antennas array for ultra-wideband near-field radar imaging," in *Proc. Eur. Conf. on Antennas Propag.*, Mar. 2012, pp. 898–901.

[9] Z. Wang, P. Hall, J. Kelly, and P. Gardner, "TEM horn circular array for wide band pattern notch reconfigurable antenna system," in *Proc. Antennas and Propag. Conf. (LAPC)*, 2010 Loughborough, Nov. 2010, pp. 365–368.

[10] W. F. Moulder, B. T. Perry, and J. S. Her, "Wideband antenna array for simultaneous transmit and receive (STAR) applications," in Proc. *IEEE Antennas Propag. Soc. Int. Symp*., Memphis, TN, USA, Jul. 2014, pp. 243–244.

[11] I. D. Longstaff and D. E. N. Davies, "A wideband circular array for H.F. communications," *Radio Electron. Eng.*, vol. 35, no. 6, pp. 321–328, Jun. 1968.

[12] M. Elmansouri and D. Filipovic, "Miniaturization of TEM horn using spherical modes engineering," *IEEE Trans. on Antennas and Propag.*, accepted.

[13] M. Elmansouri and D. Filipovic, "Omnidirectional/directional TEM horn circular array for joint time and frequency operation," in *Proc. IEEE Antennas Propag. Soc. Int. Symp. (APSURSI)*, Vancouver, BC, Jul. 2015, pp. 2205–2206.

[14] G. Marrocco and M. Ciattaglia, "Hermite-rodriguez UWB circular arrays," *IEEE Trans. Antennas Propag.*, vol. 58, no. 2, pp. 381–390, Feb. 2010.

[15] M. Malek and M. Hussain, "Antenna patterns of nonsinusoidal waves with the time variation of a Gaussian pulse: Part I," *IEEE Trans. Antennas Propag.*, vol. 30, no. 4, pp. 504–512, Nov. 1989.

[16] D. S. Filipović and T. P. Cencich, "Frequency independent antennas," in *Antenna Engineering Handbook*, 4th ed., ch. 13, New York, NY, USA: McGraw-Hill, 2007.

[17] Mini circuits Inc., NY, USA. Available online: http://www.minicircuits.com/pdfs/ZN8PD1-63W+.pdf.

[18] C. Roblin, "Representation, Characterization, and Modeling of Ultra Wide Band Antennas," in *Ultra Wide Band Antennas*, ch. 3, NJ: John Wiley, 2011.

[19] C.–H. Liao, P. Hsu, and D.–C. Chang, "Energy patterns of UWB antenna arrays with scan capability," *IEEE Trans. on Antennas and Propag.*,vol. 59, no. 4, pp. 1140–1147, April 2011.

[20] H. Sheng, P. Orlik, A. M. Haimovich, L. J. Cimini, and J. Zhang, "On the spectral and power requirements for ultra-wideband transmission," in *Proc. IEEE Int. Conf. Communications*, Mar. 2003, vol. 1, pp. 738–742.